Scripta METALLURGICA Vol. 22, pp. 1873-1878, 1988
Printed in the U.S.A.

A FURTHER CONTRIBUTION TO THE PHASE CONSTITUTION IN $(Fe_{0.65}Mn_{0.35})_{0.83}Al_{0.17}$-xC PSEUDO-BINARY SYSTEM

K. H. Han*, W.K. Choo+ and D. E. Laughlin

Department of Metallurgical Engineering and Materials Science
Carnegie Mellon University
Pittsburgh, PA 15213, USA

*On leave of absence from Department of Metallurgical Engineering
Yeungnam University, Gyongsan, Kyongbuk, Korea

+Department of Materials Science and Engineering
Korea Advanced Institute of Science and Technology
Cheongryang, P.O. Box 131, Seoul, Korea

(Received August 10, 1988)
(Revised September 23, 1988)

Introduction

The austenitic Fe-Mn-Al-C alloys (1,2) which do not contain strategic elements have received increasing interest recently. This is due to their potential importance based on attractive properties such as good oxidation resistance at elevated temperatures (2,3), excellent age hardening (4-7) and low temperature mechanical behaviour (8). In spite of many recent investigations on these alloys (9), the phase constitution in the Fe-Mn-Al-C quaternary system has not been well explored. This lack of information on phase stability of the alloys at elevated temperatures prompted Choo and Han to perform a phase diagram study (10) of $(Fe_{0.65}Mn_{0.35})_{0.83}Al_{0.17}$-xC pseudo-binary alloys (x = 0 to 16 at.%) prepared by the melt spinning technique.

Fig. 1 reproduces the quasi-equilibrium phase diagram of the $(Fe_{0.65}Mn_{0.35})_{0.83}Al_{0.17}$-xC pseudo-binary alloys determined by Choo and Han (10). This work was the first to show how the solubility of the κ carbide, $(Fe,Mn)_3AlC_x$ ($L'1_2$ structure) in the austenite (γ) varies with temperature and carbon content. It is seen that the solubility decreases rapidly with decreasing temperature. The technological importance of this result arises from the fact that the age hardening in Fe-Mn-Al-C alloys is known (4-7) to occur during the decomposition of the supersaturated γ phase which forms the κ carbide. More specifically, it was shown previously (6,7,11) that the best hardening is attained for these alloys when the aging is performed at lower temperatures to induce the formation of {100} modulated structures during the initial decomposition. The initial decomposition occurring under these conditions ("pre-precipitation") is believed (11) to proceed *via* the spinodal process (12). It becomes apparent from the above mentioned facts that information about the region of the phase diagram where the modulated structures occur is important. This information would give a better understanding of metastable phase constitution and also would help in the designing of age-hardenable alloys based on the Fe-Mn-Al-C system. Unfortunately, no systematic work has been devoted to this subject. For this reason, we have performed this study extending previous work (10) to investigate the limiting temperature for the formation of modulated structures as a function of the carbon content using the $(Fe_{0.65}Mn_{0.35})_{0.83}Al_{0.17}$-xC pseudo-binary alloys.

Experimental

We utilized the melt-spun pseudo-binary alloys (Table 1) which consisted of a single austenitic phase as determined by X-ray diffraction patterns (10). The aging treatments were performed between 823 and 1113 K for various times up to 1.6×10^3 s to determine the region of the phase diagram where the modulated structure is obtained. Two kinds of salt baths were used for heat treating: 50%$NaNO_2$-50%KNO_3 (for aging below 923 K) and 20%NaCl-25%KCl-55%$BaCl_2$ (for aging above 983 K). In particular, in the case of aging at higher temperatures where the aging time was less than or equal to 120 s, the melt-spun alloys were directly dipped into the salt baths after wrapping them in copper foils. Otherwise, the melt-spun alloys were sealed in evacuated pyrex tubes prior to their aging treatments. Structural examination was carried out by X-ray diffraction, scanning electron microscopy (SEM) and transmission electron microscopy (TEM). The details of the experimental procedures were described elsewhere (10,11,13).

0036-9748/88 $3.00 + .00

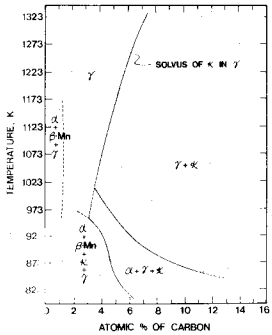

Figure 1.

Quasi-equilibrium phase diagram of $Fe_{0.65}Mn_{0.35})_{0.83}Al_{0.17}$-xC pseudo-binary alloys. Reproduced from Ref. 10.

TABLE 1. Composition of $(Fe_{0.65}Mn_{0.35})_{0.83}Al_{0.17}$-xC Pseudo-Binary Alloys* Used in This Study

Alloy No.	Composition (wt.%)				
	Fe	Mn	Al	C At.%(=x)	C (Wt.%)
1	Bal.	31.7	8.9	3.0	0.74
2	Bal.	31.6	8.9	4.0	0.98
3	Bal.	31.5	8.9	5.0	1.23(1.234)**
4	Bal.	31.5	8.8	5.5	1.36
5	Bal.	31.4	8.8	6.5	1.62(1.651)**

* Melt-spun ribbons of 25 to 33 μm in thickness.

** Values in parentheses are analyzed compositions for the melt-spun ribbons.

Results and Discussion

All the melt-spun alloys revealed an apparently homogeneous austenitic grain structure with the grain size ranging from 1 to 10 μm (Fig. 2) except for alloy no.1 (3 at.%C). The latter revealed a fine-scale cellular solidification structure with a cell spacing of about 0.2 to 1 μm. After the aging experiments, however, similar cellular segregation was observed inside the austenite grains of each of the alloys, as described below.

Two types of diffuse intensity were observed in the X-ray diffraction patterns depending on the aging temperature. Fig. 3 shows the {200} reflection and accompanying diffuse intensity taken from alloy no. 4 (5.5 at.%C) aged at 993 and 1071 K. Sidebands are seen to flank the main Bragg reflection of the parent γ phase for the sample aged at 993 K. This type of diffuse intensity was observed for all aging temperatures lower than this one. On aging at higher temperatures, distinct sidebands no longer appeared. Instead, another type of diffuse intensity appeared, characterized by an asymmetric broadening of the main Bragg peak (see Fig. 3-b). In the case of alloy no. 1, however, only the line broadening type of diffuse intensity could be observed at aging temperatures as low as 773 K.

To investigate the microstructural features responsible for the two types of diffuse intensity observed at different aging temperatures, TEM examination was performed. Figs. 4a and 4b show the bright field TEM images, of the same specimens of alloy no. 4 that had been studied by X-ray diffraction (Figs. 3a and 3b, respectively). Comparing Figs. 4-a and 3-a it is seen that,

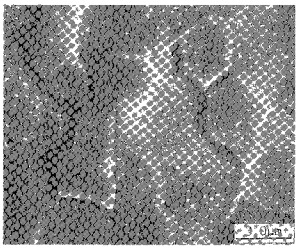

Figure 2

Scanning electron micrograph of melt-spun alloy no. 5, 6.5 at% C.

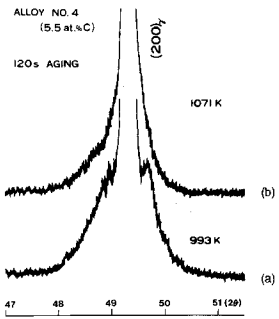

Figure 3

X-ray diffraction profiles around the $(200)_\gamma$ Bragg reflections showing the change in the type of diffuse intensity with the aging temperature.

as expected from the phenomenological diffraction theories (15,16), the sidebands arose from a modulated (periodic) structure that formed uniformly throughout the grains. Calculation of the modulation wavelength using the Daniel-Lipson (15) formula and the average angular separation between the sideband intensity maxima and main Bragg peak yielded a value of 24 nm. The observed modulation wavelength (≈ 23 nm) in Fig. 4-a was in good agreement with this value calculated from the x-ray pattern. This is consistent with the previous concomitant observation of the sidebands (satellites) and modulated structure for conventionally prepared Fe-Mn-Al-C alloys (11). In that work (11), it was judged, from the observed extinction of the satellite pairs appearing around different fundamental reflections in the selected area electron diffraction patterns, that the formation of the satellites was mainly caused by lattice parameter modulations.

On the other hand, at higher aging temperatures where the diffuse intensity appeared only as asymmetric line broadening (see Fig. 3-b) a peculiar non-uniform microstructure was observed as can be seen from Fig. 4-b. It is noted from this micrograph that the aged specimen still contained a modulated structure but some regions of the matrix were not transformed. Also, the modulation

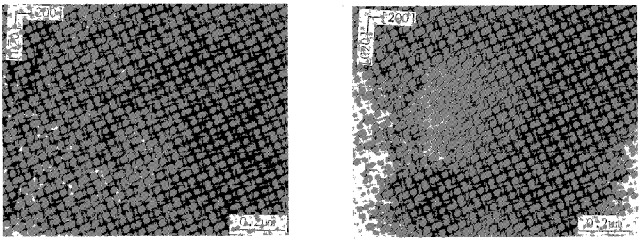

(a) (b)

Figure 4

Bright field transmission electron micrographs of alloy no. 4 showing the change of the aged microstructure with the temperature: (a) 993 K, 120 s, (b) 1071 K, 120 s. Taken from the same specimens that had been used for X-ray diffraction (Fig. 3). Foil normals near [002].

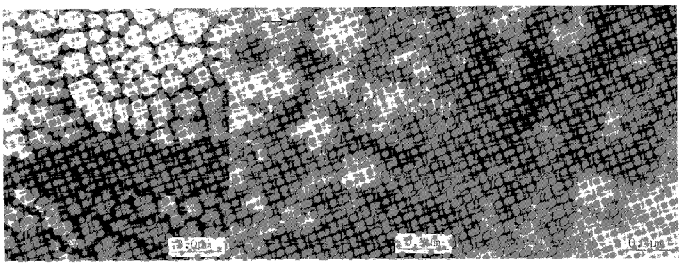

(a) (b) (c)

Figure 5

Bright field TEM of alloy no. 1 (3 at.%C) showing the preferential formation of the modulated structure along the intercellular regions of solidification segregation. (a) low magnification; (b) and (c) two beam conditions with g_{020} and g_{220}, respectively. Foil normals of (b) and (c) near [002].

was not as regular as that shown in Figure 4-a. A similar microstructure was also observed for alloy no. 1 (Fig. 5) which revealed a fine cellular solidification structure and only line broadening in the x-ray pattern on aging. Fig. 5 clearly shows that the formation of such a non-uniform microstructure is related to the cellular segregation during solidification, giving rise to a non-uniformity in local

solute composition inside the austenite grains. This in turn implies that the melt-spun alloys, having appeared to be apparently homogeneous austenitic structure (Fig. 2), also contained some solute segregation.

From Figs. 4-b and 5 it can be deduced that the cell boundary regions were richer in solute (e.g. C) than the innercell regions since decomposition occurred only in the former regions. Thus the limiting temperature for the formation of the modulated structure was higher in the cell boundary regions than in the inner cell regions. In addition, as noted above, the modulated structure formed under these aging conditions was far less periodic (especially in those regions near the untransformed matrix) than the structure formed at lower temperatures.

Figure 6 summarizes the X-ray and TEM results, for decomposition of melt spun alloys. Below the solid line, the alloys decompose *uniformly* into solute enriched and solute depleted regions. This is the modulated structure exemplified in Fig. 4-a. Just above the solid line, alloys are not sufficiently supersaturated to uniformly decompose. Regions depleted in solute (inner cellular regions) do not decompose, because their supersaturation is insufficient. These results were plotted in the quasi-equilibrium diagram of Fig. 1 to compare with the solvus of the κ-carbide in the γ phase. This is shown in Fig. 7. It can be noted from the figure that the region of completely modulated structure lies far below the solvus of the κ carbide. Also, it is interesting to note that the two curves show a similar temperature dependence on carbon composition, implying that the phase involved in the modulated structure is related to the κ phase.

In summary, we have determined approximately the limit of the modulated structure in the $(Fe_{0.65}Mn_{0.35})_{0.83}Al_{0.17}$-xC pseudo-binary system and showed that the formation of the modulated structure depends on the degree of carbon supersaturation in the γ phase. We believe that this limit of modulated structure determined can be a useful guide to design high strength age-hardenable alloys based on the Fe-Mn-Al-C quaternary system. The observed change in the type of diffuse reflections from the sidebands to asymmetric line broadening can be explained in terms of the relaxation of the interference between the zone complexes of carbon-rich and carbon-poor zones due to their lessened periodicity. More detailed results on this subject and the sideband observations will be published elsewhere.

Acknowledgement

We express appreciation for the financial support of this research provided by the Korea Science and Engineering Foundation and the National Science Foundation Grant DMR-84-13115 at CMU.

References

1. J.L. Ham and R.E. Cairns, *Product Eng.* **29**, 59 (1958).
2. D.J. Schmatz, *Trans. ASM* **52**, 898 (1960).
3. J.C. Garcia, N. Rosas and R.J. Rioja, *Metal Progr.* **122**, 47 (1982).
4. P.J. James, *J. Iron Steel Inst.* **207**, 54 (1969).
5. G.L. Kayak, *Met. Sci. Heat Treat.* (2), 95 (1969).
6. G.S. Krivonogov, M.F. Alekseyenko and G.G. Solov'yeva, *Phys. Met. Metallogr.* **39**, 86 (1975).
7. K.H. Han, W.K. Choo, D.Y. Choi and S.P. Hong, *Proceedings of the Symposium on Alternate Alloying for Environmental Resistance*, Louisiana, 1986, Ed. by G.R. Smolik and S.K. Banerji, TMS-AIME, 91 (1987).
8. J. Charles, A. Berghezan, A. Lutts and P.L. Dancosine, *Metal Progr.* **118**, 71 (1981).
9. For example, papers in *Proceedings of the Symposium on Alternate Alloying for Environmental Resistance*, Louisiana, 1986, Ed. by G.R. Smolik and S.K. Banerji, TMS-AIME, 91 (1987).
10. W.K. Choo and K.H. Han, *Metall. Trans.* **16A**, 5 (1985).
11. K.H. Han, J.C. Yoon and W.K. Choo, *Scripta Met.* **20**, 33 (1986).
12. J.W. Cahn, *Acta Met.* **10**, 179 (1962).
13. K.H. Han and W.K. Choo, *Metall. Trans.* **14A**, 973 (1983).
14. N.A. Storchak and A.G. Drachinskaya, *Phys. Met. Metallogr.* **44**, 123 (1977).
15. V. Daniel and H. Lipson, *Proc. Roy. Soc.* **A181**, 368 (1943).
16. E. Biedermann, *Acta Cryst.* **13**, 650 (1960).

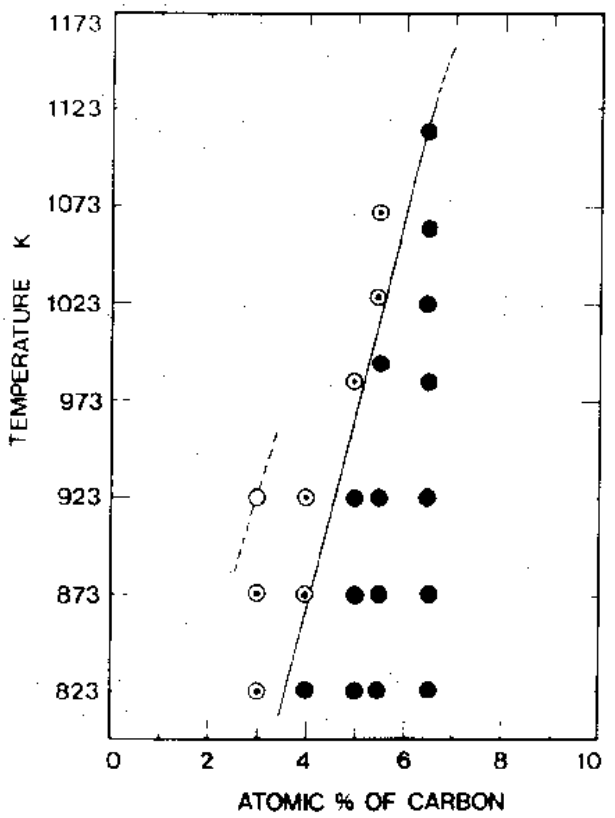

Figure 6

Diagram showing the region of modulated structure, based on X-ray diffraction and TEM.

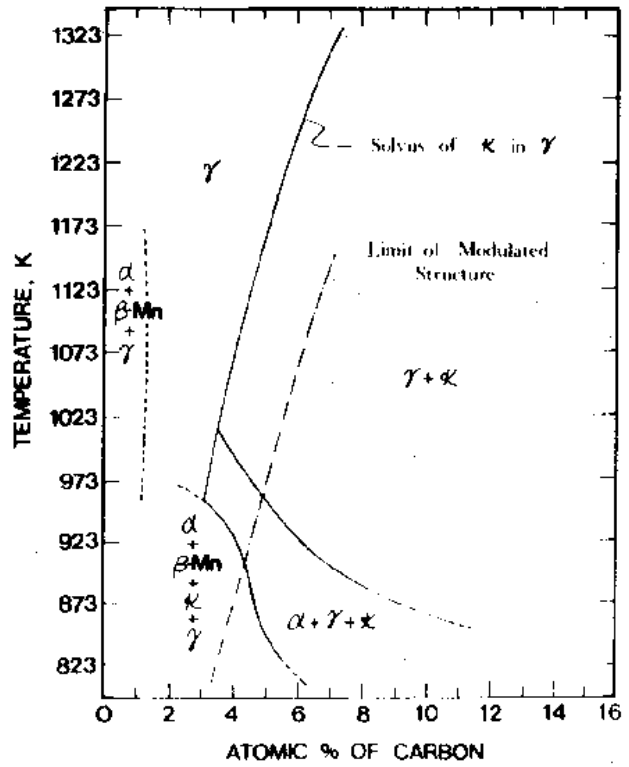

Figure 7

Comparison of the solvus of the κ carbide in γ and the limit of modulated structure determined in this study.